CrossMark

ORIGINAL PAPER

Landslide characteristics in the area of Xiaolin Village during Morakot typhoon

Y. C. Deng[1] · F. Tsai[2] · J. H. Hwang[1]

Abstract Xiaolin, a small village in southern Taiwan, was completely buried by a deep-seated landslide during the extreme rainfall of Typhoon Morakot in 2009, and 500 people were killed. This disaster caused great public concern. This study examines the rainfall-induced landslide characteristics in the area and their correlations with various susceptibility factors. We emphasize the importance of producing an accurate landslide inventory using visual interpretation and propose a new systematized set of subcategories of susceptibility factors, especially stream factors. We used satellite images, digital elevation models, and landslide inventories from before and after the disaster to perform spatial analysis using geographic information system (GIS) tools. Of the topographical factors considered, only slope aspect was important, and the landslides bore little relation to tectonic lines. The stream factors had the strongest influence on these landslides. Almost 100 % of the landslide area was related to various types of erosion caused by the stream network. Most of the large-scale landslides were induced by headward erosion, and all occurred on dip or oblique slopes. Thus, a combination of dip or oblique slope types and stream factors resulted in more landslides, which suggests that landslides are often induced by a combination of multiple factors.

Introduction

On 7–10 August 2009, Typhoon Morakot made landfall in Taiwan. It brought strong southwesterly winds and extremely heavy rainfall. Hourly rainfall exceeded 50 mm/h, with an accumulated total of more than 2500 mm. The extreme duration and intensity of the rainfall caused many landslides in the mountainous area near the village of Xiaolin. This village was completely destroyed and buried by debris from a deep-seated landslide, resulting in the loss of 500 lives. Figure 1 shows satellite images of the area before and after the landslide. This was the most serious landslide tragedy in the history of Taiwan and caused great public concern. The aim of this research is to improve understanding of landslide characteristics in the Xiaolin area by means of statistical analysis of various factors that may have influenced the landslide.

Producing a landslide inventory

An accurate landslide inventory is crucial for the initiation of a study of this type. Three methods for producing a landslide inventory are generally recognized: visual interpretation, automatic interpretation, and semi-automatic interpretation. Visual interpretation (Dai et al. 2003; Korup 2005b; Dominguez-Cuesta et al. 2007; Borgomeo et al. 2014; Chen et al. 2014) is usually conducted by hand by landslide experts, using aerial photographs or satellite images. When it is verified by means of careful field investigation, this method can produce a fairly precise landslide inventory.

✉ J. H. Hwang
  jinhunghwang@gmail.com

1 Department of Civil Engineering, National Central University, Taoyuan, Taiwan

2 Center for Space and Remote Sensing Research, National Central University, Taoyuan, Taiwan
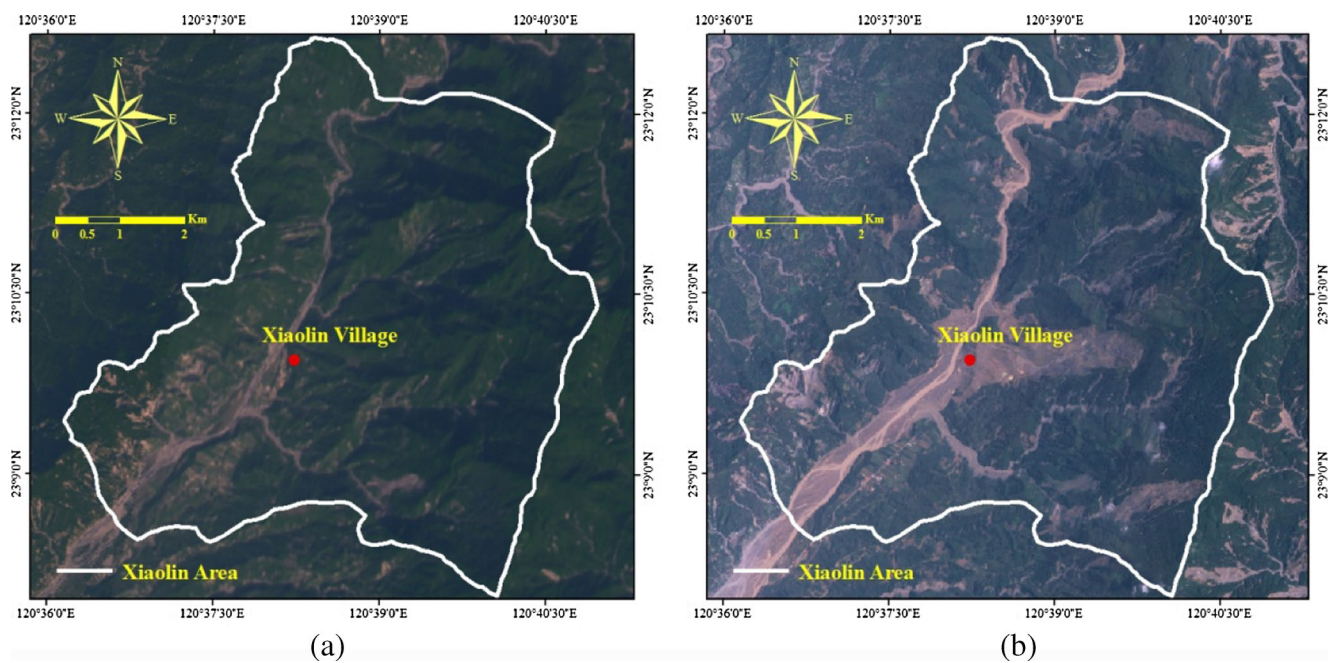
Fig. 1 **a** Pre- and **b** post-disaster satellite images of the Xiaolin area

Although visual interpretation can identify the relevant landslide details, it is a very time-consuming approach. Automatic interpretation (Malamud et al. 2004; Nichol and Wong 2005; Borghuis et al. 2007; Lee 2009) can greatly improve the efficiency of landslide inventory generation by detecting spectral and/or spatial differences between pre- and post-disaster satellite images. Because it uses only spectral characteristics and no other information, this method is however unable to produce inventories of high precision.

The semi-automatic method (Martha et al. 2010; Tsai et al. 2010; Wan et al. 2014; Mondini and Chang 2014) combines the spectral characteristics of images and other, manually obtained useful information to interpret the landslide. It can increase the accuracy of the inventory relative to the automatic method, but interpretation takes more time.

To improve the accuracy of the statistical analysis of landslide characteristics in the Xiaolin area, this study reconstructs the landslide inventory for this area based on careful visual interpretation by an experienced geotechnical engineer.

Statistics of landslide characteristics

Studies involving the statistics of landslide characteristics can be classified into two groups. The aim of one group (Dominguez-Cuesta et al. 2007; Lee et al. 2008a; Lee et al. 2008b; Vorpahl et al. 2012; Alkhasawneh et al. 2014; Chue et al. 2015; Yusof et al. 2015; Demir et al. 2015; Kayastha 2015) is to set up statistical models to identify the weights of different susceptibility factors. These studies are summarized in Table 1, which shows the susceptibility and triggering factors considered, the statistical models used, and the major influencing factors identified.

The other group (Panikkar and Subramanyan 1996; Zhou et al. 2002; Dai et al. 2003; Avanzi et al. 2004; Korup 2005a; Korup 2005b; Paudel et al. 2007; Guzzetti et al. 2008; Msilimba and Holmes 2010; Tsai et al. 2010; Goswami et al. 2011; Lin et al. 2011; Weng et al. 2011; Wu et al. 2011; Broothaerts et al. 2012; Rose 2013; Borgomeo et al. 2014; Chen et al. 2014; Kim et al. 2014; Regmi et al. 2014; Zhang et al. 2014; Chen 2015; Mansour et al. 2015) correlates the characteristics of landslides, such as slide number, area, and volume, to various susceptibility factors, such as topography, geology, stream system, vegetation, and anthropogenic source. The common practice is to feed digital maps of the landslide inventory and various susceptibility factors into a Geographic Information System (GIS) to carry out spatial analysis. Table 2 summarizes currently available studies of this kind and gives the researchers, the study area, and the susceptibility factors considered. All of these studies have made important contributions to our understanding of landslide characteristics. Since this study belongs to the second category, the preliminary results with respect to the correlation of landslide characteristics with various susceptibility factors from the above studies are summarized below.

Landslide characteristics

Most of the above studies (Hovius et al. 1997; Malamud et al. 2004; Korup 2005a; Korup 2005b; Guzzetti et al. 2008; Msilimba and Holmes 2010; Tsai et al. 2010; Goswami et al. 2011; Lin et al. 2011; Wu et al. 2011; Broothaerts et al. 2012;

Table 1 Weighting factors used in studies modeling landslide susceptibility

Publication	Susceptibility and triggering factors used	Important influencing factors
Dominguez-Cuesta et al. (2007)	Aspect, slope gradient, terrain curvature, present landslide presence, quaternary cover presence, lithology and vegetation.	Aspect, slope gradient, lithology.
Lee et al. (2008a)	Lithology; slope gradient; slope aspect; terrain roughness; slope roughness; total curvature; local slope height; total slope height; topographic index; distance from a road, a fault, a river head, and a river bend; NDVI; and maximum rainfall intensity.	Primary factors: slope gradient, NDVI; secondary factors: lithology, slope aspect, terrain, slope roughness, total curvature, total slope height.
Lee et al. (2008b)	Lithology; slope gradient; slope aspect; terrain and slope roughness; total curvature; local slope height; total slope height; topographic index; distance from a road, a fault, a river head, and a river bend; NDVI; and maximum Arias intensity.	Primary factors: slope gradient, terrain roughness, Arias intensity and lithology; secondary factors: slope aspect, slope roughness, total curvature.
Vorpahl et al. (2012)	Elevation, slope gradient and aspect, stream power index (SPI), topographic wetness index (TWI), convergence index (CI), topographic position index (TPI).	Generation region: TPI, SPI; transport region: TPI, SPI, slope gradient; deposition region: CI, TWI, SPI, TPI.
Chue et al. (2013)	Slope gradient and aspect, elevation, geology, effective accumulative rain (EAR), land disturbance, distance from river, slope roughness	Geology, slope aspect, EAR
Alkhasawneh et al. (2014)	Elevation, slope gradient and aspect, diagonal length, plan curvature, profile curvature, general curvature, tangential curvature, cross-section curvature, longitudinal curvature, surface area, surface roughness, rugosity.	Slope gradient and aspect
Yusof et al. (2015)	Elevation, slope gradient, slope aspect, slope curvature, SPI, TWI, terrain roughness index (TRI), and river factors	Elevation, SPI, TWI, TRI, river factors
Demir et al. (2015)	Elevation; slope gradient; slope aspect; distance to streams, roads, and faults; drainage density; and fault density	Elevation; slope gradient; slope aspect; distance to streams, roads, and faults, drainage density; and fault density
Kayastha (2015)	Slope aspect; slope gradient; slope curvature; relative relief; geology; distance to faults, land cover, and streams; and annual rainfall	Slope aspect; slope gradient; slope curvature; relative relief; geology; distance to faults, land cover, and streams; and annual rainfall

Chen and Huang 2013; Dahl et al. 2013; Chen et al. 2014; Borgomeo et al. 2014; Regmi et al. 2014; Chen 2015) investigated the size of the landslide area (the frequency-area distribution) and the number of landslides in their study area. Although the size definitions vary among researchers, most of them define large-scale landslides as >10 ha and small-scale as <10 ha, a definition retained by the present study.

Topographic factors

The topographic factors considered are slope gradient, slope aspect, elevation, elevation difference between adjacent valleys, local relief, and terrain curvature. Many studies (Panikkar and Subramanyan 1996; Zhou et al. 2002; Dai et al. 2003; Avanzi et al. 2004; Korup 2005b; Paudel et al. 2007; Tsai et al. 2010; Lin et al. 2011; Broothaerts et al. 2012; Rose 2013; Borgomeo et al. 2014; Kim et al. 2014; Zhang et al. 2014; Mansour et al. 2015) compared the gradient of the hillslope before the slide with the gradient of the landslide area. Most landslides have a slope gradient of 25–40°. Some studies conclude that slope gradient has significant impact on landslides, but others do not support this conclusion. Most studies show that landslides often occur on specific slope

aspects, but a few suggest that aspect has little impact. Many studies find that elevation and terrain curvature are not directly related to landslide characteristics.

Geological factors

The geological factors considered include lithology, type of overburden soil, tectonic lines, and the attitude of rock formations. Discussions of lithology are usually based on geological maps, outcrops of the rock layer, geological age, and geomechanical behavior. Most of the above studies conclude that landslides are closely related to lithology. However, this conclusion is questionable because these studies do not compare the lithology of the landslide with that of the background area. Tectonic lines are defined as faults and lineaments. Panikkar and Subramanyan (1996) used distance to fault or lineament as an index to investigate the influence of tectonic lines on landslides and showed that distance to a fault has a strong influence. The same conclusions were also reached by Korup (2005a), Guzzetti et al. (2008), Kirschbaum et al. (2010), Goswami et al. (2011), and Mansour et al. (2015).

Avanzi et al. (2004) classified slopes into downslope, oblique slope, and upslope, according to rock formation

Table 2   Studies of the statistical relationships between susceptibility factors and landslide characteristics

Publication	Study area	Important influencing factors
Panikkar and Subramanyan (1996)	Dehradran and Mussoorie region, India.	Lithology, distance to the active fault, slope gradient, slope aspect, stream erosion and NDVI.
Zhou et al. (2002)	Lantau Island, Hong Kong.	Slope gradient, elevation, vegetation.
Dai et al. (2003)	Tung Chung region, Lantau Island, Hong Kong.	Slope gradient, elevation, slope aspect, slope shape, lithology, vegetation.
Avanzi et al. (2004)	Cardoso, Mulina and Turrite di Gallicano basins, northwestern Tuscany (storm event on 19 June 1996).	Lithology, attitude of the rock layer, slope surface, slope gradient, type of overburden soil.
Korup (2005a)	Western Southern Alps and Fiordland, southwestern New Zealand.	Lithology, tectonic lines, seismic history, local relief, stream erosion.
Korup (2005b)	Western Southern Alps and Fiordland, southwestern New Zealand.	Slope gradient and slope aspect.
Paudel et al. (2007)	Subcatchments of the Sakurakigawa and Furuegawa watersheds, Japan.	Slope gradient, soil layer and lithology, slope curvature, stream presence.
Guzzetti et al. (2008)	Upper Tiber River basin, central Italy.	Lithology, attitude of the rock layer, elevation, slope gradient.
Msilimba and Holmes (2010)	Ntchenachena and Chiweita regions, northern Malawi.	High slope angle, weathered bedrock, vegetation, cumulative rainfall.
Tsai et al. (2010)	Goaping River basin, southern Taiwan. (Typhoon Morakot).	Stream erosion, slope gradient.
Goswami et al. (2011)	Eastern Peloritani, NE Sicily, and western Aspromonte, SW Calabria, Italy.	Fault activity, stream incision, climate
Lin et al. (2011)	Southern Taiwan (Typhoon Morakot).	Lithology, slope gradient.
Weng et al. (2011)	Near the Baolai Hot Spring, Laolong River basin, Taiwan (Typhoon Morakot).	Lithology, attitude of the rock layer.
Wu et al. (2011)	Chishan, Laolong, Zhuokao and Yiliao watersheds, Goaping River basin, Taiwan (Typhoon Morakot).	River bank erosion.
Broothaerts et al. (2012)	Gilgel Gibe catchment, southern Ethiopia.	Lithology, type of overburden soil, rainfall intensity, slope gradient, distance to river, stream incision.
Rose (2013)	Te Whanga Station, north Island, New Zealand	Slope gradient.
Borgomeo et al. (2014)	Molise area, central Italy.	Lithology, fluvial incision
Chen et al. (2014)	Shenmu watershed, central Taiwan.	Tectonic faults, River bank erosion
Kim et al. (2014)	Pyeongchang area, Korea (Typhoon Ewiniar).	Slope gradient, slope aspect, slope curvature, vegetation.
Regmi et al. (2014)	Paonia–McClure Pass study area, western Colorado, USA.	Slope gradient, slope curvature, slope length-width ratio
Zhang et al. (2014)	Milestone K1 to K45 of Province Road 303, Wenchuan county, Sichuan province, China (storm event on 14 August 2010).	Elevation, internal relief, slope gradient, lithology
Mansour et al. (2015)	Ouarsenis area, western Algeria.	Tectonic faults, road, lithology, slope aspect, slope gradient.

attitude and slope aspect, and found that most landslides occur on downslopes. Guzzetti et al. (2008) and Weng et al. (2011) reached the same conclusion, but Panikkar and Subramanyan (1996) found that rock formation attitude was not a major influencing factor on the landslides in their study.

Stream factors

The stream factor considers the influence of streams and rivers on landslides. A useful index is distance to the nearest river. Both Wu et al. (2011), Broothaerts et al. (2012), Chen et al. (2014) and Borgomeo et al. (2014) reported this as an important factor because of stream erosion at the toe of the slope. The studies that have considered stream factors (Panikkar and Subramanyan 1996; Avanzi et al. 2004; Korup 2005a; Tsai et al. 2010) all found

them to be highly important in determining susceptibility to landslides and concluded that most landslides are induced by headward erosion. Despite the importance of this factor, no systematic categorization of its effect has however been developed yet.

Objective

While all of the above studies have made significant contributions to understanding landslides, there is still room for improvement particularly with respect to the following issues: (a) the influence of the accuracy of the landslide inventory; (b) dominant susceptibility factors for small- vs. large-scale landslides; (c) systematical identification of patterns of stream erosion that influence landslides; (d) the effects of rock formation attitude and tectonic lines;

and (e) the influence of a compound susceptibility factor. Consideration of these issues may make future studies more rigorous.

The aim of this study was to improve our understanding of the characteristics of landslides in the Xiaolin area that were induced by the most serious Typhoon Morakot and to identify the major factors determining susceptibility to these landslides, using more rigorous data and methods. For the purposes of constructing a highly accurate landslide inventory using visual interpretation by a professional geotechnical engineer and because of time constraints, the study area was reduced to a small area surrounding the Xiaolin village. Maps of the various susceptibility factors and landslides in the area were overlaid in ArcGIS 9.2 for visual interpretation and analysis.

Materials and methods

Xiaolin is located in Jiasian District, Kaohsiung City, southern Taiwan (Fig. 1). The area belongs to the western foothills geological zone, and the regional geology is rather complicated (Fig. 2). The geological formations include the Hunghwatzu formation (thick-bedded siltstone and alternation of thick siltstone and sandstone), Yenshuikeng shale (massive shale), Tangenshan sandstone (thick-bedded sandstone and muddy sandstone), the Changchikeng formation (alternation of sandstone and shale), terrace deposits, and recent alluvium. The Xiaolin syncline passes the high river terrace east of Xiaolin village. The strike of the fold axis runs north-northeast to south-southwest (NNE-SSW), and the dip runs towards the south. Part of the area is dip slope. The Chiahsien fault passes through the east side of the syncline at a distance of about 800–900 m. Two kilometers eastward, another major fault, the Chishan, passes through the area. The Xiaolin area has many fractured zones as a result of various geological structures (e.g., the syncline and the faults).

The primary materials we used to identify landslides were Formosat-2 satellite images, a digital elevation model (DEM), and an inventory of Morakot-induced landslides from Tsai et al. (2010). The satellite images had been corrected by Tsai et al. (2010) by means of orthorectification and radiometric correction. The pre-disaster satellite images were acquired on 14 and 15 January 2009, and the post-disaster images were acquired on 17 August 2009. We used a pre-disaster DEM of the whole study area, with a resolution of 40×40 m, and a post-disaster DEM of the largest landslide area (the Xiaolin slide), with a resolution of 5×5 m. The inventory of Morakot-induced landslides (Fig. 3) was originally generated by Tsai et al. (2010) using the semi-automatic method, by detecting changes in NDVI computed from the pre- and post-disaster satellite images.
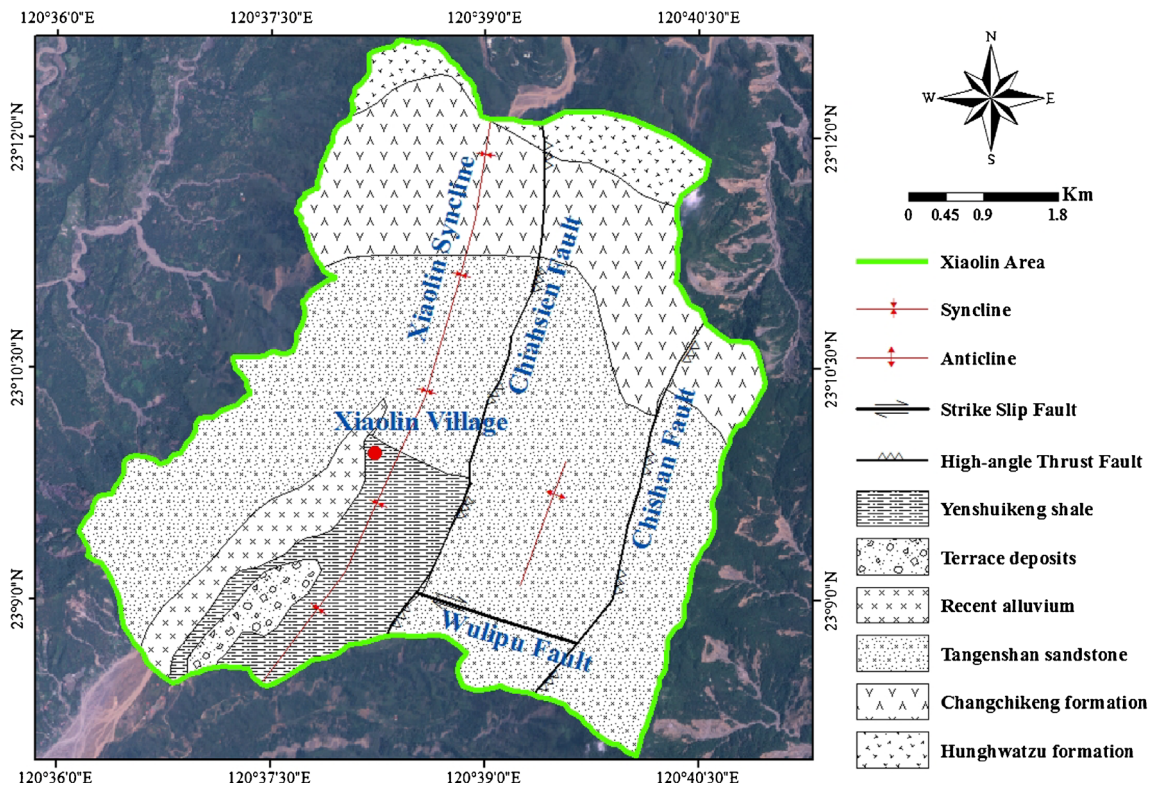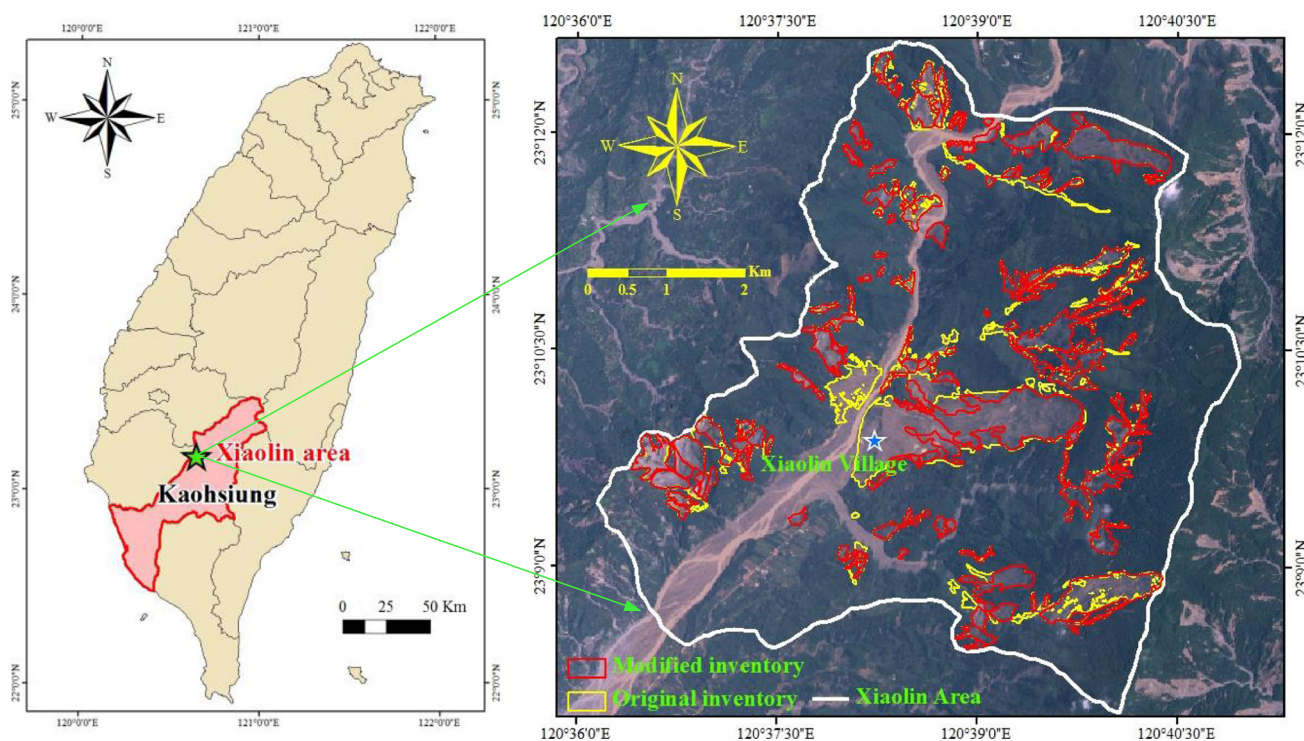

Fig. 2 Geological map of the Xiaolin area

(a) Map showing the location of Xiaolin in Taiwan.   (b) Original and modified landslide inventories.

Fig. 3 Original and modified landslide inventories

Examination and correction of landslide inventory

The original landslide inventory had some commission and omission errors as a result of the use of automation in change detection analysis. There were three kinds of errors in the original inventory: (i) vegetated area was found in the interpreted landslide area; (ii) the interpreted large slide may actually have consisted of several smaller slides; and (iii) the deposit area of the landslide was incorrectly interpreted as part of the landslide area, causing the area and volume of the landslide to be overestimated. We therefore reexamined the original inventory and corrected it based on the Formosat-2 satellite images, Google Earth images from 17 November 2001 and 29 January 2010, and maps of slope gradient and aspect from ArcGIS 9.2.

We used the 3D-view option in Google Earth to check whether the interpreted large landslide area actually consisted of several smaller slides. This allowed clarification of slide area and direction as well as enabled estimation of the deposit area and its removal from the slide area as interpreted by the automatic method.

To check the area of the Xiaolin landslide (the largest of the Typhoon Morakot-related landslides, which destroyed the village), we obtained and analyzed high resolution (5 × 5 m) pre- and post-disaster DEMs. The resulting map (Fig. 4) shows the differences in elevation between the two DEMs. The red areas denote a negative elevation difference

and represent the slide area. The green areas denote a positive elevation difference and represent the deposit area. Based on this analysis, the area of the Xiaolin landslide, assessed as 227 ha in the original inventory, was approximately halved to 113 ha. This demonstrates the importance of subtracting the deposit area from the estimated landslide area.

Deposit areas are often found to rest on gentle or extremely gentle slopes. We therefore used an empirical criterion suggested by Franks (1999) that parts of the slide area located on slopes less than 10° be regarded as deposit areas and deducted from the original slide area.

Finally, before we statistically analyzed the landslide characteristics, we reassessed the number of landslides. The original landslide inventory defined interconnected areas with pixels showing similar spectral reflectance (signifying landslides) as a single landslide. However, this definition often results in a single large landslide area that includes several smaller slides induced by different streams and slopes. It is thus difficult to assess the compound factors involving flow direction and slope aspect that would have influenced the sliding mechanism of these component landslides. We propose defining a single landslide based on the relationship between slide and flow directions. We call the inventory created using this definition a detailed landslide inventory, which contains a larger number of landslides than the original one (Fig. 3).
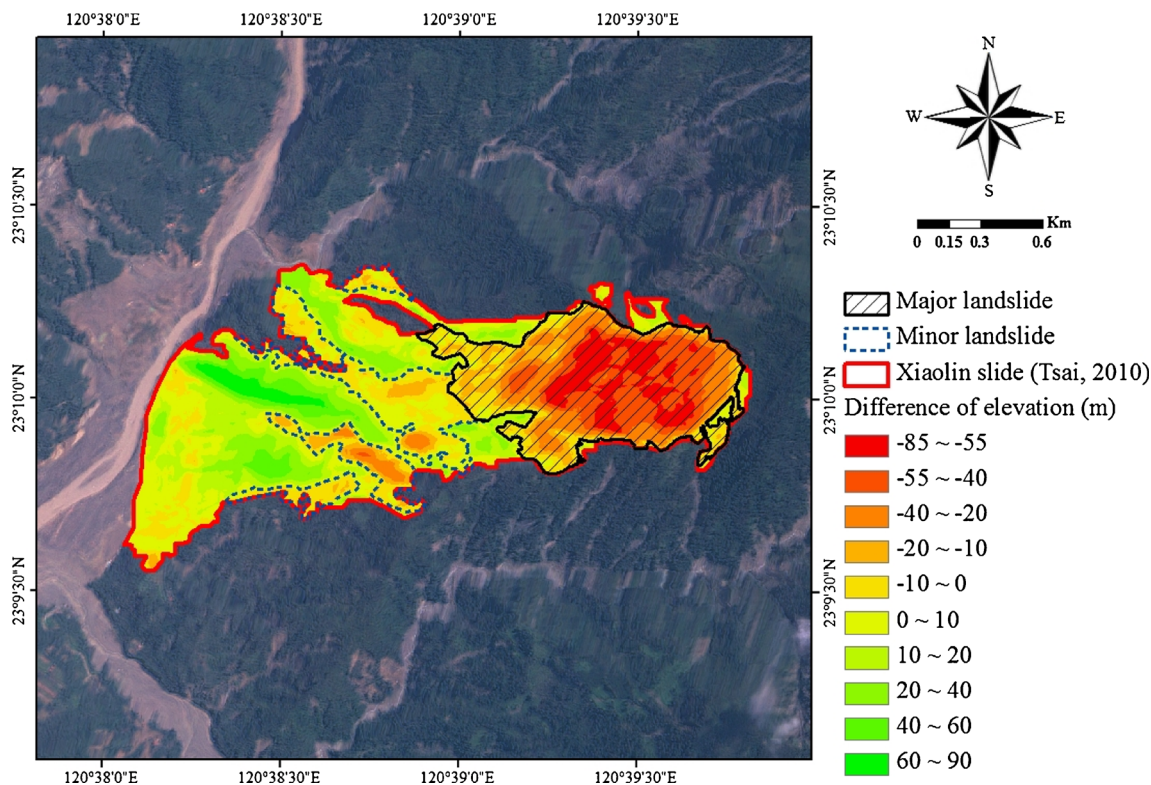
Fig. 4 Elevation difference between pre-disaster and post-disaster DEMs

Generating maps of susceptibility factors

We used ArcGIS 9.2 and the pre-disaster DEM with a resolution of 40 × 40 m to calculate the stream-related factors and topographic susceptibility factors. The stream-related factors considered were stream presence, stream erosion, and stream order (Fig. 5a). These were mainly generated using the hydrology module in ArcGIS 9.2 and carefully modified manually to correct some unreasonable results. The topographic factors were elevation (Fig. 5b), slope aspect (Fig. 5c), and slope gradient (Fig. 5d), which were obtained using the spatial analyst module in ArcGIS 9.2. Data about lithology, tectonic lines, and the attitude of the rock layers were obtained from the Central Geological Survey in Taiwan.

Statistical index and subcategories of susceptibility factors

The landslide characteristics we considered were the number and area of landslides. Landslides of different scales may have different sliding mechanisms as a result of varying geological, hydrological, and topographical conditions. We classified landslides as large-scale if they were larger than 10 ha in area and as small-scale otherwise.

To understand the size distribution of the landslides, we calculated and analyzed two indices: (i) the ratio of the number of landslides of each size class to the total number of landslides; and (ii) the ratio of the total area of landslides of each size class to the total area of all the landslides. These two ratios are formulated as below:

$$\text{Number ratio} = \frac{\text{number of small or large landslides}}{\text{total number of landslides}} \times 100\%$$

$$(1)$$

$$\text{Area ratio} = \frac{\text{total area of small or large landslides}}{\text{total area of all landslides}} \times 100\%$$

$$(2)$$

To investigate the effects of the different susceptibility factors on these landslide characteristics, we compared the indices of these factors for the landslide area against those for the background area. For each subcategory of a susceptibility factor, we calculated the area or number of a subcategory in the total landslide area as a proportion of the total landslide area/number, and the area/number of that subcategory in the background area as a proportion of the total background area/number of hillslopes. These two ratios were calculated as follows:

Landslide area ratio for a subcategory

$$= \frac{\text{landslide area of a subcategory}}{\text{total area of landslides}} \times 100\% \qquad (3)$$
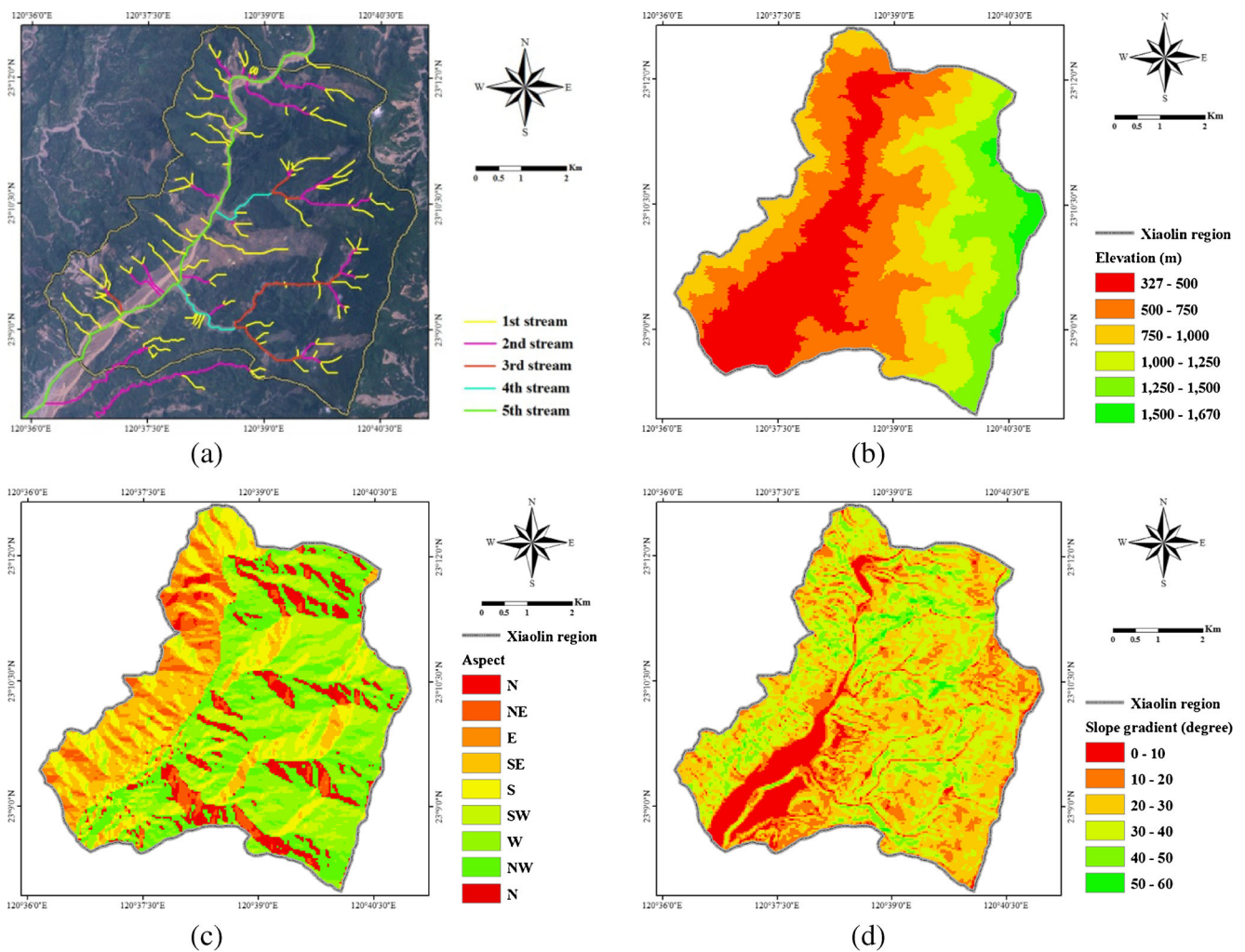
Fig. 5 Susceptibility factors in the study area: **a** stream and stream order; **b** elevation; **c** aspect; **d** slope gradient

Background area ratio for a subcategory

$$= \frac{\text{background area of a subcategory}}{\text{total background area}} \times 100\%$$

(4)

Subcategories of susceptibility factors

The topographical factors we considered were slope elevation, aspect, and gradient. We calculated their average value for each landslide using the spatial analyst module in ArcGIS 9.2. Elevation was divided into the following subcategories: (I) 0–500 m; (II) 500–1000 m; (III) 1000–1500 m; and (IV) 1500–2000 m. Slope gradient was divided into the following: (I) 0–10°; (II) 10–20°; (III) 20–30°; (IV) 30–40°; (V) 40–50°; and (VI) > 50°. Finally, slope aspect was divided into eight orientations: N; NE; E; SE; S; SW; W; and NW.

The geological factors we included were lithology, tectonic lines, and slope type. We classified the lithology of the area into the following: (I) Hunghwatzu formation; (II) Yenshuikeng shale; (III) Tangenshan sandstone; (IV) Changchikeng formation; (V) terrace deposits; and (VI) recent alluvium (Fig. 2). The tectonic lines we considered were faults and folds. Following Lee et al. (2000), a line's influence zones were assumed to extend 150 m either side of its surface traces. This factor was classified into four types: (I) fault without fold; (II) fold without fault; (III) both fault and fold; and (IV) neither fault nor fold. We also divided this factor into two broader categories according to the presence or absence of a tectonic line.

Slope type is defined by the relationship between the attitude of the rock layer and the aspect of the slope. According to the Technical Manual of Water and Soil Conservation in Taiwan, slopes are classified into three types: dip slope, escarpment slope, and oblique slope. Dip slopes have the highest risk of sliding. If the slip plane does not daylight,

i.e., run at a shallower angle than the slope face, the risk is lower.

Stream factors have the strongest influence on landslides because of their undercut and erosion effect on the toe of a slope. The aspects of stream factors that we investigated were the stream erosion, stream order, and stream presence. The stream presence factor is the simplest and was classified into two states: presence or absence of a stream. Based on the geometric relationships between streams and slides, we classified the landslides into five types according to their relationship with stream erosion: (I) slides induced by gully erosion; (II) slides induced by headward erosion; (III) slides induced by bank scouring and side erosion; (IV) slides induced by slope undercutting; and (V) landslides not related to streams (Table 3, Fig. 6).

Based on Strahler (2010), stream order was classified into six types: (I)–(V) first to fifth order streams; and (VI) landslides not related to streams. The lower the stream order, the upper the stream.

Landslides may occur as a result of one or more susceptibility factors. We therefore tentatively investigated two kinds of compound factors. The first encoded the relationship between stream direction and slope aspect. This factor was divided into four subcategories: (I) stream flow and aspect orientations within 45° of each other; (II) orientations differing by 45–90°; (III) orientations differing by 90–135°; and (IV) landslides not related to streams (Fig. 7). The second compound factor was a combination of slope type and stream presence. This factor was classified into six categories as follows: (I) dip slope with stream; (II) dip slope without stream; (III) escarpment slope with stream; (IV) escarpment slope without stream; (V) oblique slope with stream; and (VI) oblique slope without stream. The influence of these compound factors on the landslide characteristics was calculated directly by overlapping the maps of the relevant susceptibility factors, using ArcGIS 9.2.

Results and discussion

Landslide characteristics in the Xiaolin area

Total study area (background area) was 4005 ha, and total landslide area, comprising 144 separate landslides, was 623.9 ha (Table 4). Although there were only 16 large-scale slides, they contributed 57.3 % of the total landslide area. In contrast, there were 128 small-scale slides, which occupied 42.7 % of the total landslide area. Thus, the number of landslides was not necessarily positively correlated with total landslide area, as a result of different sliding mechanisms. Lin et al. (2011); Tsai et al. (2010); Wu et al. (2011); Chen and Huang (2013); Chen et al.(2014), and Chen (2015) reported similar findings in Taiwan area. Hovius et al. (1997); Malamud et al. (2004); Korup (2005a, 2005b); Guzzetti et al. (2008); Goswami et al. (2011); Broothaerts et al. (2012), Dahl et al. (2013); Borgomeo et al. (2014), and Regmi et al. (2014) reported similar findings all around the world.

Distributions of topographical and geological susceptibility factors

Since the number of landslides was not positively correlated with total landslide area, we compared both the number and area ratios for the various susceptibility factors between the landslide and background areas, to assess their influence on the landslide characteristics (Fig. 8). The following subsections discuss the correlations between these susceptibility factors and the landslide characteristics.

Elevation factor

Both the largest number and area ratios were found in the elevation range of 500–1000 m, and there were no landslides in the range of 1500–2000 m (Fig. 8a). However, the ratios were similar for both the landslide and the background areas. Thus, elevation does not seem to have been a major

Table 3 Definition of landslides in relation to stream erosion

| Type	Description
I: gully erosion	Landslides caused by side and upward erosion in the small gullies of a stream's uppermost reaches. This type of erosion does not induce large headward slides (Fig. 6a).
II: headward erosion	Landslides caused by erosion of the stream bed at the head of the stream, which causes the toe of the slope behind the river head to be removed and the slope to collapse. The head of the river thus extends gradually upwards, and often triggers large-scale landslides (Fig. 6b).
III: bank scouring and side erosion	Landslides caused by this type of erosion are restricted to the river bank as a result of the scouring of the toe of bank slopes or erosion of the banks (Fig. 6c).
IV: undercutting slope	Landslides caused by this type of erosion are restricted to the concave side of a river bend, and occur as a result of the direct attack and scour of river flow (Fig. 6d),
V: landslides not related to streams	These landslides are unrelated to stream systems (Fig. 6e).
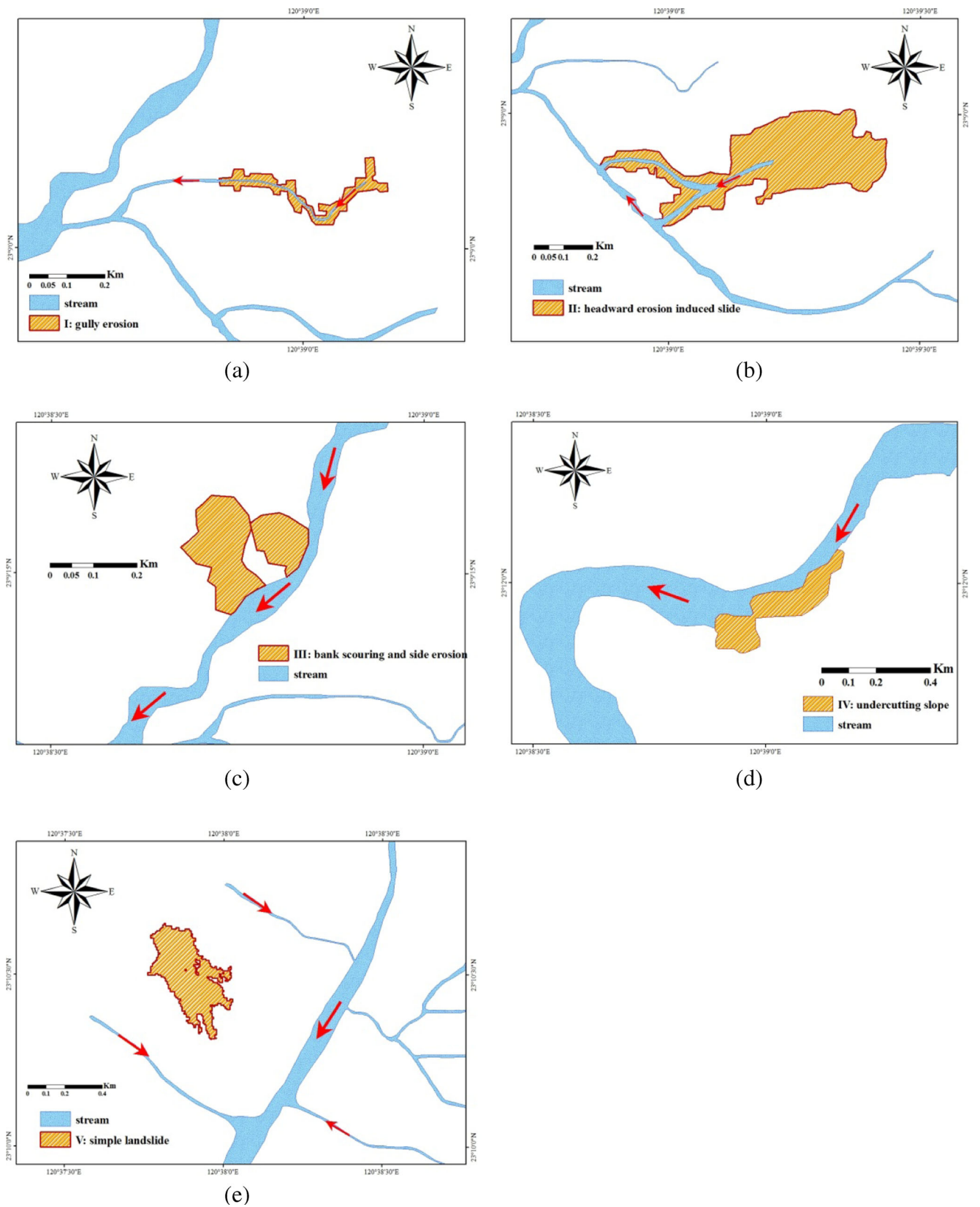
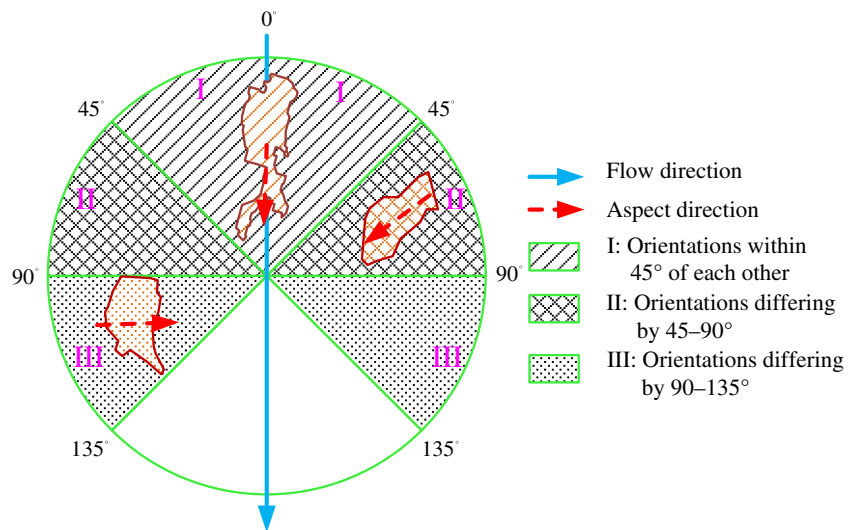**Fig. 6** Landslides induced by the following types of erosion: **a** *I*, gully erosion; **b** *II*, headward erosion; **c** *III*, bank scouring and side erosion; **d** *IV*, undercutting slope; **e** *V*, landslide not related to stream erosion

Fig. 7 Combinations of orientations of stream flow direction and slope aspect

susceptibility factor. This conclusion is consistent with those of Panikkar and Subramanyan (1996), Tsai et al. (2010), and Broothaerts et al. (2012). However, Dai et al. (2003) and Guzzetti et al. (2008) indicated the elevation factor is unable to be neglected.

Slope gradient

No landslides occurred in steep areas (slope gradient >50°; Fig. 8b). Most landslides occurred on slopes of 20–40°, with a lower number ratio but higher area ratio for slides on slopes of 20–30°. Since the number and area ratios for gradient were however also similar for both the landslide and the background areas, gradient cannot be a major susceptibility factor. Korup, O. (2005b), Lin et al. (2011), Tsai et al. (2010) and Borgomeo et al. (2014) reached similar conclusions; however, Panikkar and Subramanyan (1996), Zhou et al. (2002), Dai et al. (2003), Paudel et al. (2007), Guzzetti et al. (2008), Msilimba et al. (2010), and Mansour et al. (2015) pointed out the slope gradient has a substantial influence on landslides.

Slope aspect factor

The area ratio for landslides on west-facing slopes was much higher than that of the background area of slopes of that aspect (Fig. 8c). In other words, the percentage of the area of west-

facing slopes that was subject to landslides was substantially larger than for other slope aspects. There were few slides on slopes facing northeast and almost none on north-facing slopes. The predominance of landslides on west-facing slopes is a result of the fact that most stream directions in the area run in an east-west direction. The streams thus induce headward erosion primarily on west-facing slopes. In this area, this is therefore an important factor affecting landslide susceptibility. This conclusion is unusual for the Taiwan area because of a lack of understanding of the underlying relationship between slope aspect and stream direction. Although Panikkar and Subramanyan (1996), Korup (2005b), Kim et al. (2014) and Mansour et al. (2015) have indicated the slope aspect is an important factor, they did not explain the underlying relationship that found in the research.

Lithology

The highest ratios were concentrated on the Tangenshan sandstone and Changchikeng formations (Fig. 8d). There were no landslides on the terrace deposit or recent alluvium formations because of their gentle slopes. The ratios for all formations were similar for the landslide and background areas, so we are unable to directly conclude that lithology is an important factor in determining landslide susceptibility here. However, lithology should be an important factor in a large study area

Table 4 Characteristics of the landslides in the Xiaolin area

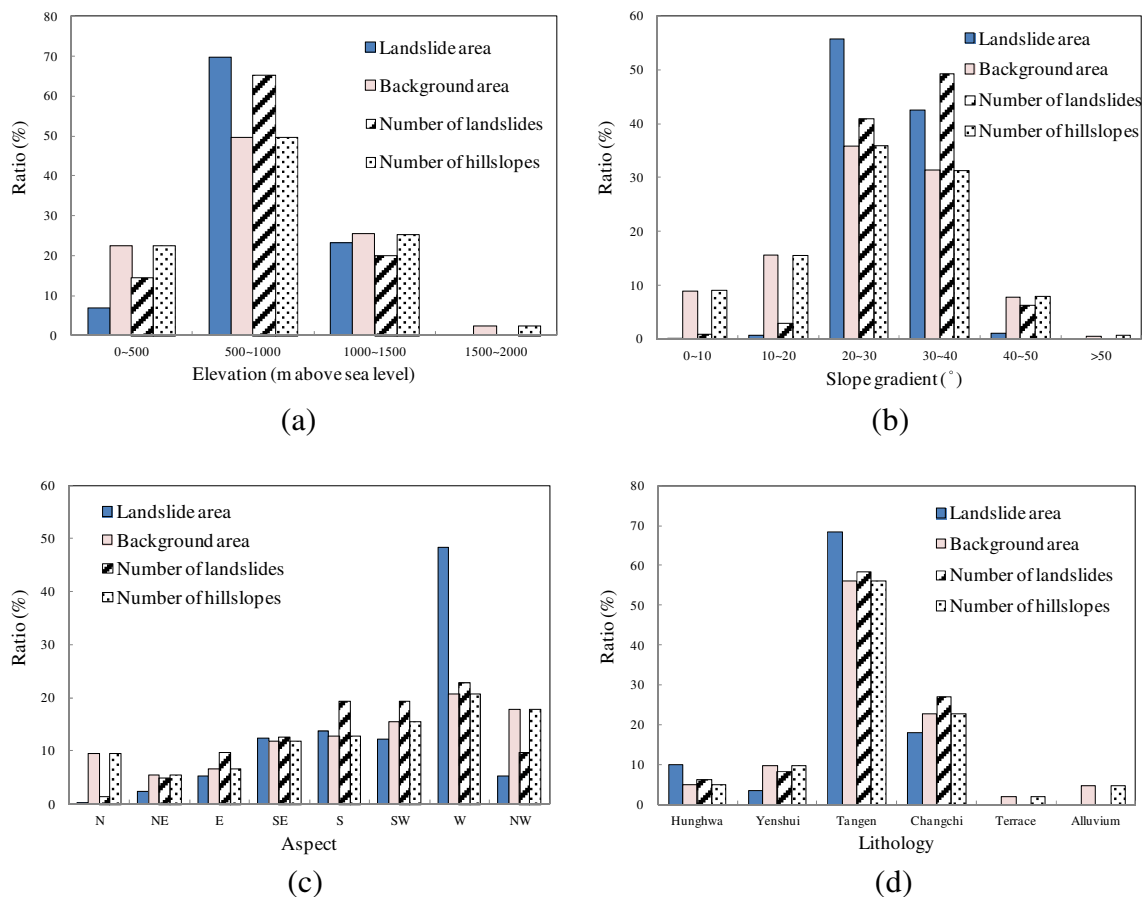| Size class	Number of landslides	Total area (ha)	Proportion of total number (%)	Proportion of total area (%)
Large (>10 ha)	16	357.6	11.1	57.3
Small (<10 ha)	128	266.3	88.9	42.7

Fig. 8 Number and area ratios of susceptibility factors to landslide and background areas: **a** elevation; **b** slope gradient; **c** slope aspect; **d** lithology

consisting of different kind of formations. This conclusion has been confirmed by Panikkar and Subramanyan (1996), Dai et al. (2003), Avanzi et al. (2004), Korup (2005a), Guzzetti et al. (2008), Msilimba et al. (2010), Broothaerts et al. (2012), Borgomeo et al. (2014), and Mansour et al. (2015).

Tectonic lines

The regional geological map was overlaid on the landslide inventory to investigate the influence of tectonic lines, i.e., folds and faults, on the landslides (summarized in Table 5). The ratio of the number of landslides for type IV (neither fault nor fold present) was 68.8 % and that of landslide area was 58 %. Thus, most of the landslides were not strongly related to areas with tectonic lines. Only one large slide, the Xiaolin landslide, was located in an area with both fault and fold lines. Only 22.2 % of the landslides were in areas with a fault line but no fold lines (type I), and they represented 23.7 % of the total landslide area. This shows that the landslides were not closely related to faults. This is particularly the case for the large landslides, for which the respective proportions were 18.8 and 22.1 %, respectively (Table 5). Overall, this analysis shows that tectonic lines have little effect on landslides. This conclusion is very different from those of Panikkar and

Subramanyan (1996), Korup (2005a), Guzzetti et al. (2008), Kirschbaum et al. (2010), Goswami et al. (2011), Chen et al. (2014), and Mansour et al. (2015).

Stream-related factors

Type III stream erosion (bank scouring) caused the largest proportion of landslides in terms of number (43.1 %) but only the second largest in terms of area (27.3 %; Table 6). Thus, most slides that are triggered by bank scouring are small-scale. This is confirmed by the small percentage of total large-scale landslides (12.5 %) and their total area (6.8 %) caused by bank scouring. Type II erosion (headward erosion) induced 75 and 87.1 % of large-scale landslides in terms of number and area, respectively. Headward erosion is therefore strongly correlated with large-scale landslides. Landslides that were not related to streams comprised 6.9 % of the total number of slides but only 0.7 % of the total area. Thus, most of these landslides were small-scale, presumably because their sliding mechanisms were not related to stream factors.

Most of the landslides occurred in the vicinity of first order streams (Table 7). They were thus related to the headward erosion that occurs in a stream's headwaters. No large land-slides happened near fourth order streams, and only 3.1 % of

Table 5 Relationship between tectonic lines and landslide characteristics. Values are percentages

Tectonic lines	Proportion of total number of landslides	Proportion of total landslide area	Proportion of number of large landslides	Proportion of number of small landslides	Proportion of area of large landslides	Proportion of area of small landslides
I: fault without fold	22.2	23.7	18.8	22.7	22.1	25.8
II: fold without fault	8.3	3.3	0.0	9.3	0.0	7.9
III: both fault and fold[a]	0.7	15.0	6.2	0.0	26.1	0.0
IV: neither fault nor fold	68.8	58.0	75.0	68.0	51.8	66.3

[a] The large-scale landslide is the Xiaolin landslide

the area of large slides was close to fifth order streams. This suggests that large-scale landslides often occur in the upper or middle reaches.

All of the large landslides were related to the presence of a stream, and the majority of the landslides were related to the various types of erosion caused by stream network (Table 6). We therefore conclude that factors related to stream were the most important factors determining landslide susceptibility in the Xiaolin area in 2009. This is a novel finding for this area, although there is some discussion of headward erosion in Tsai et al. (2010). Although Panikkar and Subramanyan (1996), Avanzi et al. (2004), Korup (2005a), Goswami et al. (2011), Wu et al. (2011), Chen et al. (2014) and Borgomeo et al. (2014) have revealed the stream factors are important to landslides, to the authors' knowledge, there is no such complete classification of stream erosion factors that has previously been proposed or discussed.

Compound susceptibility factors

Most of the landslides (irrespective of size) were located in areas where the orientation difference between slope aspect and stream direction was less than 90° (type I or type II; Table 8). In addition, most of the large landslides were induced mainly by headward erosion (type I), which results from the eroding or scouring of the toe of the slope in a stream's headwaters. Most landslides of type II (difference in orientations of 45–90°) were primarily caused by side erosion. The lower prevalence of type III slides (where the orientations of stream and aspect differed by 90–135°) indicates

that stream bank undercutting generally induced small landslides.

The majority of the landslides, including all the large-scale slides, occurred on dip or oblique slopes, with only a few small slides occurring on escarpment slopes (Table 9). Weng et al. (2011) found that in a neighboring area, most landslides occurred on dip slopes. The same conclusions are also reached by Avanzi et al. (2004) and Guzzetti et al. (2008). However, equal numbers of large slides occurred on both types of slopes, although the area ratio for dip slopes was 17 % higher than for oblique slopes. Many more small-scale slides occurred on oblique slopes than on dip slopes, though, both in terms of number and area. However, few landslides occurred on either dip or oblique slopes in the absence of stream. Thus, the presence of a stream is a much stronger influencing factor than the slope type.

Conclusion

Our main conclusions are summarized below.

1. Landslide inventories should exclude the runout zone from automatically interpreted landslide areas to produce a much more useful database for studying landslide characteristics.
2. Of the total study area, which is 4005 ha in extent, the total area of the landslides was 623.9 ha. Although there were only 16 large-scale slides, they accounted for 57.3 % of the total landslide area, and 128 small-scale slides accounted for the remaining 42.7 % of the area.

Table 6 Stream erosion categories in relation to landslide characteristics. Values are percentages

Stream erosion category	Proportion of total number of landslides	Proportion of total landslide area	Proportion of number of large landslides	Proportion of number of small landslides	Proportion of area of large landslides	Proportion of area of small landslides
I: gully erosion	27.1	10.3	6.3	29.7	3.0	20.1
II: headward erosion	20.8	59.2	75.0	14.1	87.1	21.7
III: bank scouring	43.1	27.3	12.5	46.9	6.8	54.9
IV: undercutting	2.1	2.5	6.2	1.5	3.1	1.6
V: landslides not related to streams	6.9	0.7	0.0	7.8	0.0	1.7

Table 7 Stream order categories in relation to landslide characteristics. Values are percentages

Stream order category	Proportion of total number of landslides	Proportion of total landslide area	Proportion of number of large landslides	Proportion of number of small landslides	Proportion of area of large landslides	Proportion of area of small landslides
I: first order stream	59.1	66.8	68.7	57.8	70.6	61.8
II: second order stream	13.2	8.3	12.5	13.3	6.8	10.3
III: third order stream	7.6	16.2	12.5	7.0	19.5	11.7
IV: fourth order stream	5.6	1.8	0.0	6.3	0.0	4.3
V: fifth order stream	7.6	6.2	6.3	7.8	3.1	10.2
VI: landslides not related to streams	6.9	0.7	0.0	7.8	0.0	1.7

Table 8 Relationship between slope aspect, stream flow direction, and landslide characteristics. Values are percentages

Slope aspect and flow direction	Proportion of total number of landslides	Proportion of total landslide area	Proportion of number of large landslides	Proportion of number of small landslides	Proportion of area of large landslides	Proportion of area of small landslides
I: orientations within 45° of each other	54.9	75.2	87.5	50.8	94.0	50.0
II: orientations differing by 45–90°	30.6	17.8	6.3	33.6	2.9	37.8
III: orientations differing by 90–135°	7.6	6.3	6.2	7.8	3.1	10.5
IV: landslides not related to streams	6.9	0.7	0.0	7.8	0.0	1.7

3. Of the topographical factors considered, only slope aspect was strongly related to landslide susceptibility; most of the slopes in the landslide area were west-facing. The predominant stream direction in the study area is east-west, which resulted in landslides on slopes with a westerly aspect because of headward erosion.

4. Neither lithology nor tectonic lines had a significant influence on the characteristics of the landslides in this study. Most of the landslides did not occur in the vicinity of tectonic lines.

5. Factors related to stream systems had the strongest influence on the landslides that occurred after the extreme rainfall event caused by Typhoon Morakot. Almost all the landslides were related to the various types of erosion associated with the stream network. Most of the large-scale landslides were closely related to headward erosion, which takes place in a stream's headwaters. The majority of the small-scale slides were related to bank scouring. The few landslides that were not related to streams were all small-scale, presumably because their sliding mechanisms were not linked to stream systems.

6. Most of the landslides, including all the large-scale slides, occurred on dip or oblique slopes, and almost none occurred on escarpment slopes. However, few landslides occurred even on dip or oblique slopes in the absence of a stream. Stream systems therefore exerted a much stronger influence on landslide susceptibility in this area than slope type.

Table 9 Relationship between slope type, stream presence, and landslide characteristics. Values are percentages

Slope type	Stream presence	Proportion of total number of landslides	Proportion of total landslide area	Proportion of number of large landslides	Proportion of number of small landslides	Proportion of area of large landslides	Proportion of area of small landslides
Dip	With stream	22.2	42.2	50.0	18.8	58.5	20.4
	Without stream	0.7	0.1	0.0	0.8	0.0	0.1
Escarpment	With stream	6.3	3.6	0.0	7.0	0.0	8.4
	Without stream	0.0	0.0	0.0	0.0	0.0	0.0
Oblique	With stream	64.6	53.5	50.0	66.4	41.5	69.5
	Without stream	6.3	0.7	0.0	7.0	0.0	1.5

References

Avanzi GD, Giannecchini R, Puccinelli A (2004) The influence of the geological and geomorphological settings on shallow landslides. An example in a temperate climate environment: the June 19, 1996 event in northwestern Tuscany (Italy). Eng Geol 73:215–228

Alkhasawneh MS, Ngah UK, Tay LT, Isa NAM (2014) Determination of importance for comprehensive topographic factors on landslide hazard mapping using artificial neural network. Environmental Earth Sciences 72(3):787–799

Borghuis AM, Chang K, Lee HY (2007) Comparison between automated and manual mapping of typhoon-triggered landslides from SPOT-5 imagery. Int J Remote Sens 28(7–8):1843–1856

Broothaerts N, Kissi E, Poesen J, Van Rompaey A, Getahun K, Van Ranst E, Diels J (2012) Spatial patterns, causes and consequences of landslides in the Gilgel Gibe catchment, SW Ethiopia. Catena 97:127–136

Borgomeo E, Hebditch KV, Whittaker AC, Lonergan L (2014) Characterising the spatial distribution, frequency and geomorphic controls on landslide occurrence. Molise, Italy, Geomorphology 226:148–161

Chen CY, Huang WL (2013) Land use change and landslide characteristics analysis for community-based disaster mitigation. Environ Monit Assess 185(5):4125–4139

Chen SC, Chou HT, Chen SC, Wu CH, Lin BS (2014) Characteristics of rainfall-induced landslides in Miocene formations: a case study of the Shenmu watershed, Central Taiwan. Eng Geol 169:133–146

Chen CY (2015) Landslide and debris flow initiated characteristics after typhoon Morakot in Taiwan. Landslides. doi:10.1007/s10346-015-0654-6

Chue YS, Chen JW, Chen YR (2015) Rainfall-induced slope landslide potential and landslide distribution characteristics assessment. J Mar Sci Technol 23(5):705–716

Dai FC, Lee CF, Wang SJ (2003) Characterization of rainfall-induced landslides. Int J Remote Sens 24(23):4817–4834

Dominguez-Cuesta MJ, Jimenez-Sanchez M, Berrezueta E (2007) Landslides in the central coalfield (Cantabrian Mountains, NW Spain): geomorphological features, conditioning factors and methodological implications in susceptibility assessment. Geomorphology 89(3–4):358–369

Dahl MPJ, Mortensen LE, Jensen NH, Veihe A (2013) Magnitude–frequency characteristics and preparatory factors for spatial debris-slide distribution in the northern Faroe Islands. Geomorphology 188:3–11

Demir G, Aytekin M, Akgun A (2015) Landslide susceptibility mapping by frequency ratio and logistic regression methods: an example from Niksar–Resadiye (Tokat, Turkey). Arab J Geosci 8(3):1801–1812

Franks CAM (1999) Characteristics of some rainfall-induced landslides on natural slopes, Lantau Island, Hong Kong. Q J Eng Geol 32:247–259

Guzzetti F, Ardizzone F, Cardinali M, Galli M, Reichenbach P, Rossi M (2008) Distribution of landslides in the Upper Tiber River basin, central Italy. Geomorphology 96(1–2):105–122

Goswami R, Mitchell NC, Brocklehurst SH (2011) Distribution and causes of landslides in the eastern Peloritani of NE Sicily and western Aspromonte of SW Calabria, Italy. Geomorphology 132(3–4):111–122

Hovius N, Stark CP, Allen PA (1997) Sediment flux from a mountain belt derived by landslide mapping. Geology 25(3):231–234

Korup O (2005a) Geomorphic imprint of landslides on alpine river systems, southwest New Zealand. Earth Surf Process Landf 30(7):783–800

Korup O (2005b) Distribution of landslides in southwest New Zealand. Landslides 2(1):43–51

Kirschbaum DB, Adler R, Hong Y, Hill S, Lerner-Lam A (2010) A global landslide catalog for hazard applications: method, results, and limitations. Nat Hazards 52(3):561–575

Kim G, Won S, Kim D (2014) GIS based analysis of landslide effecting factors in the Pyeongchang area. Journal of the Korean Society of Surveying, Geodesy, Photogrammetry and Cartography 32(3):261–269

Kayastha P (2015) Landslide susceptibility mapping and factor effect analysis using frequency ratio in a catchment scale: a case study from Garuwa sub-basin. East Nepal Arabian Journal of Geosciences. doi:10.1007/s12517-015-1831-6

Lee CT (2009) Review and prospect on landslide and debris flow hazard analysis. Journal of the Taiwan Society of Public Works 5:1–29(in Chinese with English abstract)

Lee CT, Kang KH, Cheng CT, Liao CW (2000) Surface rupture and ground deformation associated with the Chi-Chi, Taiwan earthquake. Sino-Geotechnics 81:5–18(in Chinese with English abstract)

Lee CT, Huang CC, Lee JF, Pan KL, Lin ML, Dong JJ (2008a) Statistical approach to storm event-induced landslides susceptibility. Nat Hazards Earth Syst Sci 8(4):941–960

Lee CT, Huang CC, Lee JF, Pan KL, Lin ML, Dong JJ (2008b) Statistical approach to earthquake-induced landslide susceptibility. Eng Geol 100(1–2):43–58

Lin CW, Chang WS, Liu SH, Tsai TT, Lee SP, Tsang YC, Shieh CL, Tseng CM (2011) Landslides triggered by the 7 August 2009 typhoon Morakot in southern Taiwan. Eng Geol 123(1–2):3–12

Malamud BD, Turcotte DL, Reichenbach P, Guzzetti F, Reichenbach P (2004) Landslide inventories and their statistical properties. Earth Surf Process Landf 29(6):687–711

Msilimba GG, Holmes PJ (2010) Landslides in the Rumphi District of Northern Malawi: characteristics and mechanisms of generation. Nat Hazards 54(3):657–677

Martha TR, Kerle N, Jetten V, Van Westen CJ, Kumar KV (2010) Characterising spectral, spatial and morphometric properties of landslides for semi-automatic detection using object-oriented methods. Geomorphology 116(1–2):24–36

Mondini AC, Chang KT (2014) Combining spectral and geoenvironmental information for probabilistic event landslide mapping. Geomorphology 213:183–189

Mansour Z, Miloud B, Donzé F, Soraya R, Abderahmane H (2015) Morphometric analysis of landslides in the Ouarsenis area (west Algeria): implications for establishing a relationship between tectonic, geomorphologic, and hydraulic indexes. Arab J Geosci 8(9):6465–6482

Nichol J, Wong MS (2005) Satellite remote sensing for detailed landslide inventories using change detection and image fusion. Int J Remote Sens 26(9):1913–1926

Panikkar SV, Subramanyan V (1996) A geomorphic evaluation of the landslides around Dehradun and Mussoorie, Uttar Pradesh, India. Geomorphology 15(2):169–181

Rose RCD (2013) Slope control on the frequency distribution of shallow landslides and associated soil properties, North Island, New Zealand. Earth Surf Process Landf 38(4):356–371

Regmi NR, Giardino JR, Vitek JD (2014) Characteristics of landslides in western Colorado, USA. Landslides 11(4):589–603

Paudel PP, Omura H, Kubota T, Inoue T (2007) Spatio-temporal patterns of historical shallow landslides in a volcanic area, Mt. Aso, Japan. Geomorphology 88(1–2):21–33

Strahler AN (2010) Quantitative geomorphology of drainage basins and channel network. In: Handbook of Applied Hydrology. McGraw-Hill Book Company, USA, pp 4–39 ~ 4–76

Tsai F, Hwang JH, Chen LC, Lin TH (2010) Post-disaster assessment of landslides in southern Taiwan after 2009 typhoon Morakot using remote sensing and spatial analysis. Nat Hazards Earth Syst Sci 10(10):2179–2190

Vorpahl P, Elsenbeer H, Märker M, Schröder B (2012) How can statistical models help to determine driving factors of landslides? Ecol Model 239:27–39

Wu CH, Chen SC, Chou HT (2011) Geomorphologic characteristics of catastrophic landslides during typhoon Morakot in the Kaoping Watershed, Taiwan. Eng Geol 123(1–2):13–21

Weng MC, Wu MH, Ning SK, Jou YW (2011) Evaluating triggering and causative factors of landslides in Lawnon River Basin, Taiwan. Eng Geol 123(1–2):72–82

Wan S, Lei TC, Chou TY (2014) Optimized object-based image classification: development of landslide knowledge decision support system. Arab J Geosci 7(5):2059–2070

Yusof NM, Pradhan B, Shafri HZM, Jebur MN, Yusoff Z (2015) Spatial landslide hazard assessment along the Jelapang Corridor of the North-South Expressway in Malaysia using high resolution airborne LiDAR data. Arabian Journal of Geosciences. doi:10.1007/s12517-015-1937-x

Zhou CH, Lee CF, Li J, Xu ZW (2002) On the spatial relationship between landslides and causative factors on Lantau Island, Hong Kong. Geomorphology 43(3–4):197–207

Zhang S, Zhang LM, Glade T (2014) Characteristics of earthquake- and rain-induced landslides near the epicenter of Wenchuan earthquake. Eng Geol 175:58–73